A Novel Dual-Loop Control Strategy to Improve the Power Quality of Microgrids

Lian ZHOU

College of Electrical & Information Engineering, Hunan Institute of Engineering, Xiangtan, Hunan, 411104, P.R. China

Abstract **— This paper presents a new power quality dual-loop control strategy which uses a feed-forward f-P/V-Q droop controller and a voltage-current controller for the islanded operation. The proposed droop controller calculates the required active and reactive power of microsources using errors of the frequency and the voltage amplitude, which is useful for improving the response of the output power regulation. The feed-forward f-P/V-Q droop controller forms the voltage control signal for the voltage-current controller which employs approximate decoupling control to lighten the active and reactive power decoupling for the microsources and enhance the power control precision. Simulation results demonstrate that this proposed control strategy has strong oscillation suppress ability and dynamic performance. The controller can also enhance the operation capacity of the microgrid.**

Keywords - Feedforward systems; frequency control; inverters; microgrid; power quality; voltage control

I. INTRODUCTION

With the global warming, many countries are focusing on cutting their dependence on fossil fuels and developing renewable energy [1] [2]. Under this situation, the concept of "microgrid" has been proposed to improve the ability of power grid to accept volatility distributed source [3] [4]. Microgrids can be operated parallel-connected by connecting distribution network to large power grid, which is capable of meeting local load demand independently. Microgrids can not only reduce the influence of traditional grid caused by a large number of small distributed sources, enhance the efficiency of energy utilization, but also improve the security and reliability of power system.

In recent years, the hierarchical control method for the microgrids has been studied [5-7]; two typical drooping control methods used for microsources have been studied [9-11]; a kind of virtual impedance method which uses Q-L characteristics instead of Q-V characteristics to control the output voltage of inverter has been proposed [12][13]; considering the fact that the resistance of low voltage distribution power lines is impedance, a P-V/Q-f control method has been proposed [14], which uses the active power to control voltage amplitude and uses the reactive power to control voltage frequency; a strategy for controlling a microgrid under three-phase unbalanced situation has been proposed [15]. A feed forward control for distributed generations has been indicated [16], which shows that the outer loop feed forward improves system stability.

Many drooping control strategys focus on sharing the load power for microsources and work very well, but most of them pay little attention to the dynamic voltage and frequency disturbance of microgrids. With the use of a large number of precision equipments, as well as the development of smart grid, the users are in great need of higher power quality. Though, a microgrid can meet the uninterrupted power supply needs of users, it should provide users with high-quality power supply to cater their needs in the smart grid. Furthermore, for the Consortium for Electric Reliability Technology Solutions (CERTS) microgrid, a critical component which named static switch is needed. The grid requires a lot of preparation time when it reconnect to the utility grid because the appropriate frequency, voltage amplitude and phase angle requirements must be met and the typical drooping control method does not follow the frequency and voltage amplitude [17]. If the microgrid can follow the utility grid voltage change at any time, then the preparation time and the investment costs of the hardware will be reduced.

Based on the analysis above, a power quality dual-loop control strategy for microgrids has been proposed in this paper. It can restrain oscillations in the microgrid when the microsources and loads change suddenly, and is also useful to decrease the impact current when the microgrid is connected to a distribution network.

II. THE OVERALL THOUGHT OF MICROGRID'S POWER QUALITY

To solve problems of the voltage fluctuations and frequency deviation existing in microgrids, this paper carries out a strategy about power quality dual-loop control of microgrids, as Figure1 shows. Firstly, it can calculates reactive and active power that the grid and compound voltage control signal needs through the feed-forward f-P/V-Q drooping controller by making the use of the different value between the frequency and voltage amplitude. The calculation helps improving the precision and response of the output power of microsources. Secondly, it adopts an approximate decoupling control strategy to decrease the coupling between output active and reactive power of the inverter through a capacitor voltage controller (outer loop) and an inductor current controller (inner loop). Litter output of the active and reactive power is required. So the shock of the microgrid can be prevented effectively when the microsources or loads change dramatically. It is more secure and stable to operate the grid than other control strategys. This strategy can quickly follow the real-time voltage signal

of the distribute network and avoid impulse current when the grid connected suddenly.

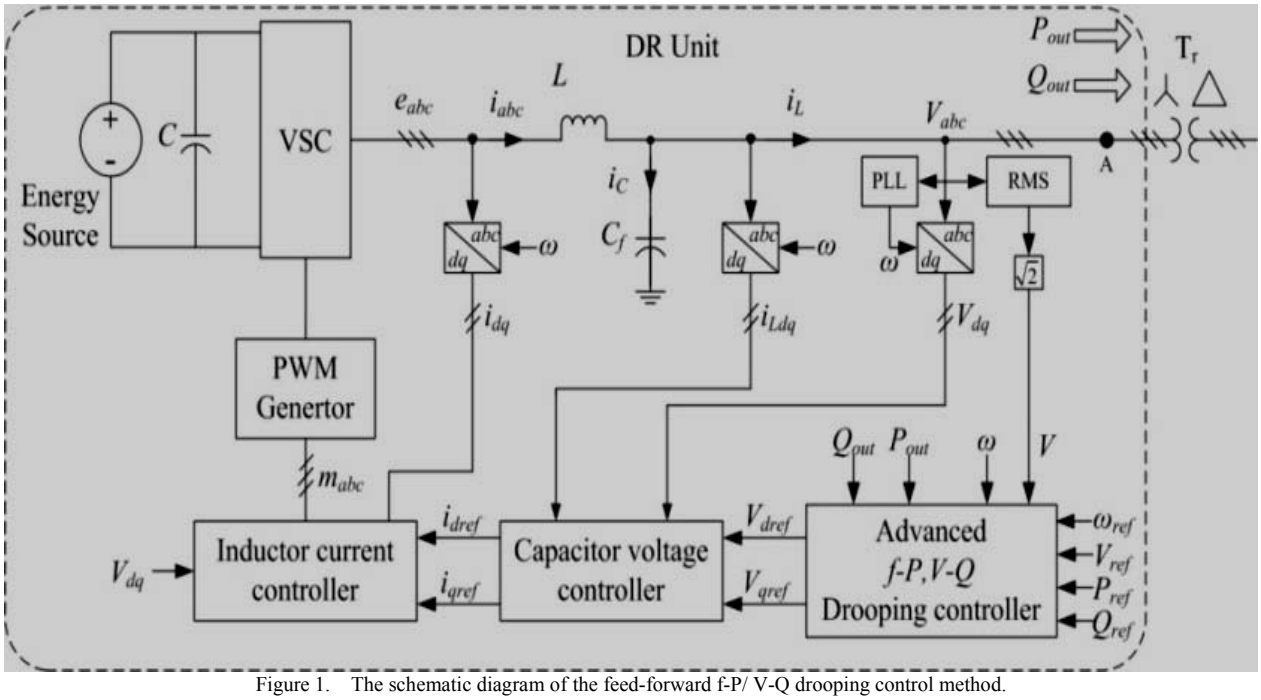

Figure 1. The schematic diagram of the feed-forward f-P/ V-Q drooping control method.

III. THE FEED-FORWARD F-P/V-Q DROOPING CONTROLLER

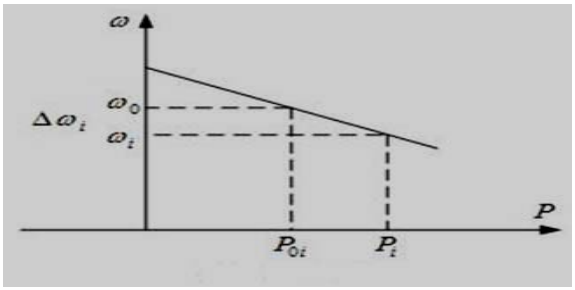

Figure 2. P-ω Drooping curve

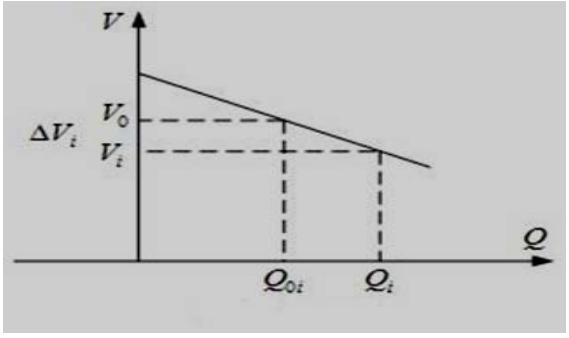

Figure 3. Q-V Drooping curve.

Figure 2 and Figure 3 show the characteristic curve of the microsource. ω_i is the set-point of frequency, ω_0 is the rated frequency and p_{0i} is the rated output power of the microsource, p_i is the actual load power, m_i is the drooping curve. It can be deduced as follows:

$$\omega_i = \omega_0 - m_i(P_{0i} - P_i) \tag{1}$$

If there is an frequency error between the rated frequency of the microgrid ω_{ref} ($\omega_{ref} = \omega_0$) and the real-time frequency of the microgrid, then:

$$\Delta\omega_i = \omega_{ref} - \omega_i \tag{2}$$

The active output power of the microsource is changed by equation:

$$\frac{dP_{0i}}{dt} = kP_{0i}\Delta\omega_i \tag{3}$$

From (1-3) the frequency dynamic error is:

$$\frac{d(\Delta\omega_i)}{dt} = m_i\frac{dP_{0i}}{dt} = m_i kP_{ir}(\Delta\omega_i) \tag{4}$$

$$\Delta\omega_i(t) = e^{km_iP_{ir}t - C} \tag{5}$$

$$\Delta\omega_i(t) = \Delta P_l \frac{1}{\sum_{j=1}^{n}\frac{1}{m_j}} e^{-t/C} \tag{6}$$

$$C = -\frac{1}{km_iP_{ir}} \tag{7}$$

It can be seen from (5) and (6) that the microgrid frequency error will finally disappear, the frequency of the microgrid will be steady in the microgrid setting frequency. The change rate is decided by the constant C, and the constant C is decided by variable k. It can quickly eliminate the microgrid frequency error and balance the system active power by setting reasonable parameters.

The connection transient between the microgrid and utility grid is more sensitive to phase mismatch and frequency mismatch than magnitude mismatch. The droop characteristic of the microsource is shiftted vertically by a small amount $\triangle d$ when changing the phase of the microgrid voltage slightly, Assuming that there is a virtual drooping controlled microsource at point A in Figure 1. The droops are now specified as follows:

$$\omega_B = \omega_0 - m_B(P_{0B} - P_B) + \Delta d \tag{8}$$

The droops of the virtual drooping controlled microsource is:

$$\omega_A = \omega_0 - m_A(P_{0A} - P_A) \tag{9}$$

At the start of the synchronization process, if $\omega_{ref} = \omega_0$ is the rated frequency of the utility grid, then:

$$\frac{d\delta}{dt} = \omega_{ref} - \omega_B = m_B(P_{0B} - P_B) + \Delta d \tag{10}$$

$$\frac{dP_B}{dt} \approx -\cos\delta_t \frac{E^2(\omega_B - \omega_A)}{\omega_0 L} \tag{11}$$

δ_t is the angle between e_{abc} and V_{abc}, assuming that δ_t approximately equal to zero, then equation (10) can be further simplified for δ_t , then:

$$\frac{d\delta}{dt} - \Delta d + \Delta d \frac{m_A(1 - e^{-t/C})}{m_B + m_A} = 0 \tag{12}$$

$$C = \frac{-\omega_0 L}{E^2(m_A + m_B)} \tag{13}$$

Equation (12) shows that the mismatch angle of phase decreases with time.

The same derivation of the droop V-Q curve can be obtained:

$$V_i = V_0 - m_i(Q_{0i} - Q_i) \tag{14}$$

$$\Delta V_i = V_{ref} - V_i \tag{15}$$

$$\frac{dQ_{0i}}{dt} = kQ_{0i}\Delta V_i \tag{16}$$

From (14) and (15) the voltage amplitude dynamic error is:

$$\frac{d(\Delta V_i)}{dt} = m_i \frac{dQ_{0i}}{dt} = m_i k Q_{0i}(\Delta V_i) \tag{17}$$

$$\Delta V_i(t) = e^{km_i Q_{0i} t - C} \tag{18}$$

$$\Delta V_i(t) = \Delta Q_l \frac{1}{\sum_{j=1}^{n} \frac{1}{m_j}} e^{-t/C} \tag{19}$$

$$C = -\frac{1}{km_i Q_{0i}} \tag{20}$$

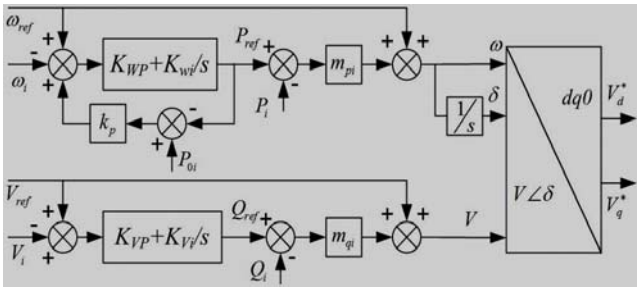

Figure 4. Block diagram of feed-forward f-P/V-Q controller.

The controller structure is shown in Figure 4. ω_{ref} is the setting frequency of the microgrid, ω_i is the real-time bus voltage frequency, P_i is the active output power of the inverter; V_{ref} is the setting voltage amplitude of the microgrid, V_i is the real-time bus voltage amplitude; Q_i is the reactive output power of the inverter. k_p and k_q are feedback gains of the f-P/V-Q controller. The parameters K_{wp} and K_{wi} are scale coefficient and Integral gain coefficient of the f-p controller respectively, K_{Vp} and K_{Vi} are scale coefficient and Integral gain coefficient of the V-Q controller respectively. Compared with previous drooping control methods [16], the advanced f-P/V-Q drooping control method adds frequency and amplitude recovery segments to improve the dynamic response by feed-forward controller. Then the voltage reference signal of the inverter is calculated by a power ring. However, the decoupling control is needed in the end of the controller to improve control accuracy because the output power coupling together.

IV. THE CAPACITOR VOLTAGE-INDUCTIVE CURRENT CONTROLLER DESIGN

The outer voltage and inner current control loops have been discussed [16]. This paper gives a detailed theoretical derivation about it in next section.

A single-phase parallel-connected equivalent circuit of the inverter is shown in Figure 1, where e_{abc} is the inverter output voltage. In other words, it is the voltage signal of the advanced f-P/V-Q drooping controller. V_{abc} is the bus voltage, C is the capacitor of the filter, L is the inductance of the filter, R is the equivalent resistance of the filter, i_{abc} is the inverter output current, i_L is the input load current of the bus, i_C is the capacitor current. So it is inferred by Kirchhoff's law as follows:

$$\begin{cases} e_{abc} = L\dfrac{di_{abc}}{dt} + i_{abc}R + V_{abc} \\ i_L + i_C = i_{abc} \\ i_C = C\dfrac{dV_{abc}}{dt} \end{cases} \tag{21}$$

It can be inferred from:

$$\begin{bmatrix} e_d \\ e_q \end{bmatrix} = \begin{bmatrix} -R & \omega L \\ -\omega L & -R \end{bmatrix} \begin{bmatrix} i_d(t) \\ i_q(t) \end{bmatrix} - L\frac{d}{dt}\begin{bmatrix} i_d(t) \\ i_q(t) \end{bmatrix} + \begin{bmatrix} V_d \\ V_q \end{bmatrix} \tag{22}$$

$$\begin{bmatrix} i_d \\ i_q \end{bmatrix} = C\frac{d}{dt}\begin{bmatrix} V_d(t) \\ V_q(t) \end{bmatrix} + \omega C\begin{bmatrix} -V_q(t) \\ V_d(t) \end{bmatrix} + \begin{bmatrix} i_{Ld} \\ i_{Lq} \end{bmatrix} \tag{23}$$

Obviously, e_d and e_q are transformed to i_{Cd}, i_{Cq} and i_d, i_q by (23) in dq0 coordinate, i_d and i_q are transformed to V_d and V_q by (22) in dq0 coordinate.

Equations are obtained as follows:

$$\begin{cases} i_d = (K_P + \dfrac{K_I}{S})(V_{dref} - V_d) - \omega C V_q + i_{Ld} \\ i_q = (K_P + \dfrac{K_I}{S})(V_{qref} - V_q) + \omega C V_d + i_{Lq} \end{cases} \tag{24}$$

$$\begin{cases} e_d = (K_P + \dfrac{K_I}{S})(i_{dref} - i_d) - \omega L i_q + V_d \\ e_q = (K_P + \dfrac{K_I}{S})(i_{qref} - i_q) + \omega L i_d + V_q \end{cases} \tag{25}$$

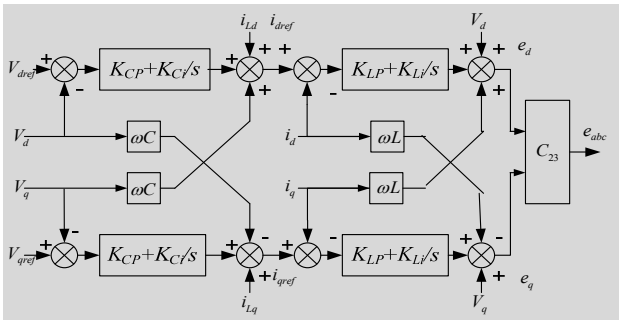

Figure 5. The schematic diagram of capacitor voltage-inductor current controller

Correspondingly, the schematic diagram of capacitor voltage (outer loop) and inductor current (inner loop) controllers are shown in Figure 5. K_{CP} and K_{Ci} are scale coefficient and integral gain coefficient of the current controller respectively. K_{LP} and K_{Li} are scale coefficient and Integral gain coefficient of the voltage controller respectively. Both of the external voltage loop and internal current loop adopt an approximate decoupling control strategy to decrease the disturbance between output active power and reactive power of inverter significantly. So the control accuracy is improved.

V. SIMULATION ANALYSIS

To verify the ability of power quality management technology for microgrid-control, a microgrid simulation model is established based on MATLAB shown in Figure 6. Microsource 1 is composed of a fuel cell and an energy storage device, using the feed-forward f-P/V-Q drooping control method; Microsource 2 is a photovoltaic device adopting maximum power point track control method; Microsource 3 is composed of a photovoltaic device and an energy storage device using PQ control method.

The microgrid system adopts 250kW as the power unit value, 380V as the bus voltage unit value. Active and reactive power setting of microsource 1 are both 0.1 unit value. The delivered power of microsource 2 is influenced by the weather conditions. The parameter of Temperature is set to 25 ℃, and light intensity is 1000 W/m^2. The active power setting of microsource 3 is set to 0.14 pu and the reactive power setting of microsource 3 is set to 0.1 p.u. Load1 is a 25kW, 25kVar constant power load. Load2 is a 50kW, 25kVar constant power load. Load3 is a 25kW constant power load. Load4 is a 50kW, 25kVar constant power load. Load5 is a 50kW, 25kVar constant power load. The parameters of the power quality dual-loop controller are given in Table 1. The parameters of the f-P/V-Q controller are according to the typical I system of Siemens "best tuning".

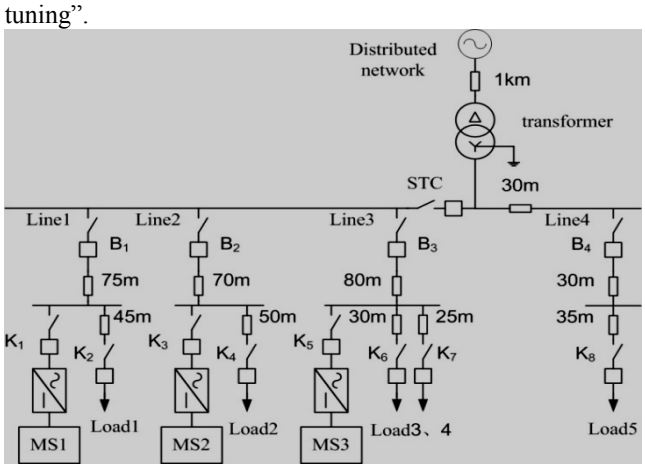

Figure 6. Typical structure of microgrid.

TABLE1. THE SIMULATION PARAMETERS ABOUT THE POWER QUALITY DUAL-LOOP CONTROL STRATEGY OF MICROGRID

Controller	Parameter	Controller	Parameter
k_p	1	k_q	0.5
K_{wp}	1	K_{Vp}	1
K_{wi}	100	K_{Vi}	100
m_{pi}	-0.0001	m_{qi}	-0.0001
K_{CP}	1	K_{LP}	1
K_{Ci}	0.1	K_{Li}	200
L	0.0005	C	0.0005

Case 1: Microgrid Starting and Response to Load Switching

At 0s, static switch is closed. B2, B3, B4, K3, K4, K5, K6 and K8 are closed. Line2, line 3 and line 4 is connected to the low voltage distribution network. Meanwhile, microsource 2 and microsource 3 begin to work. B1 is disconnected. K1 and K2 are closed and microsource 1

operations with load independently.

At 0.2s, B1 is closed. A microgrid system is built and connected to the low voltage distribution network as well as operate with it.

At 0.4s, K7 is closed. Load4 is connected to the grid.

The voltage of the microgrid bus is illustrated in Figure 7 and Figure 8. The output power of microsources is shown in Figure 14, Figure 15 and Figure 16.

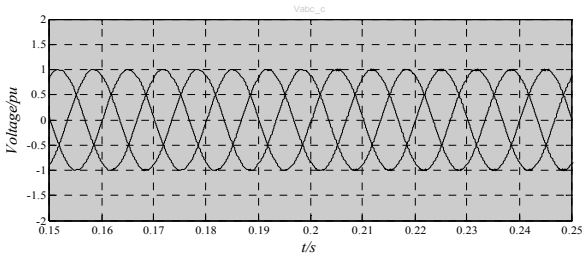

Figure 7. The voltage at the microgrid bus in case 1at 0.2s

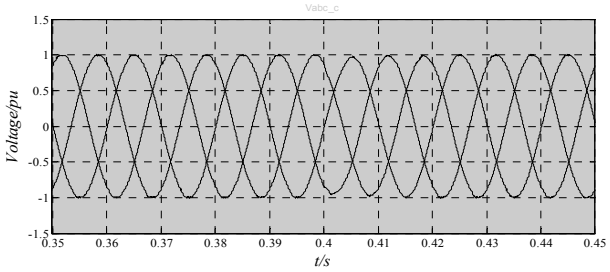

Figure 8. The voltage at the microgrid bus in case 1at 0.4s

As Figure 7 shows, when the microgrid system is built and connected to distribution in 0.2s, the power of microsource 1 slightly increases and there is no voltage fluctuation. When load4 is grid connected in 0.4s, as Figure 8 shows, the output power of microsource 1 rises rapidly and there is a slight voltage fluctuation. However, under the proposed control, the microsources remain stable.

Case 2: Transition to the Islanded Mode and Response to Power Fluctuating

At 0.6s, static switch is opened. The microgrid is disconnected from the low voltage distribution network and operated islanded.

At 0.8s, light intensity increases significantly to 1300 W/m^2, which increases the delivered power of the microsource 3.

At 1s, K7 is opened and load4 is disconnected from the grid.

As Figure 9 indicates, when the microgrid is operated islanded in 0.6s, the power of microsource 1 increases slightly. There is no impact on current, no voltage fluctuation, and no impulse current. Figure 10 shows that when the power of microsource 2 increases in 0.8s, microsource 1 responds rapidly and cuts down the output. The power of microgrid is balanced quickly and there is no voltage fluctuation. When load4 is disconnected from the grid in 1s, the output of the microsource 1 is cut down and the bus voltage rises slightly and then keeps steady after one and a half power cycle, as Figure 11 shows.

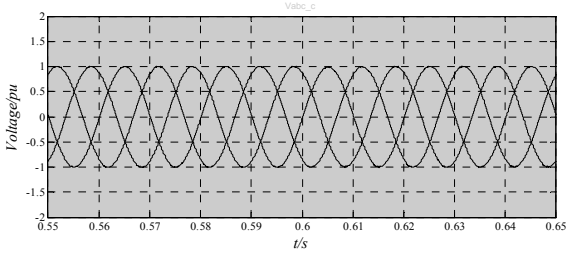

Figure 9. The voltage at the microgrid bus in case 2 at 0.6s

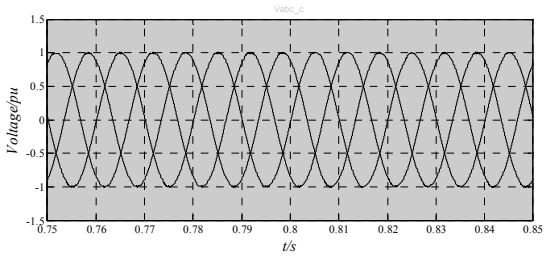

Figure 10. The voltage at the microgrid bus in case 2 at 0.8s

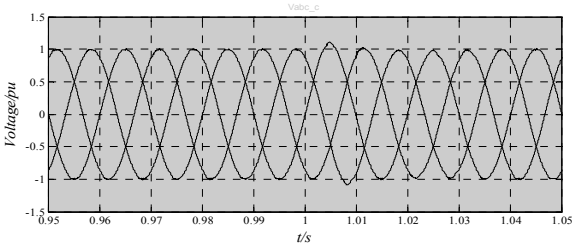

Figure 11. The voltage at the microgrid bus in case 2 at 1.0s

Case 3: Transition to the Grid-connected Mode

At 1.2s, the static switch is closed. The microgrid is connected to the distribution network again.

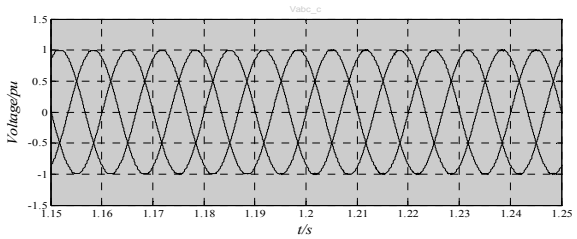

Figure 12. The voltage at the microgrid bus in case 3

Figure 12 shows that the microgrid system is built and connected to the distribution network when the static switch is closed in 1.2s. There is no voltage fluctuation. The current in static switch increases gradually and reaches to its maximum after two power cycle. So it can avoid producing impulse current, as shown in Figure 13.

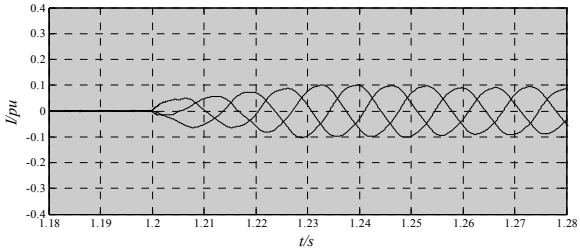

Figure 13. The current of static switch.

Microsource 1 adopts feed-forward f-P/V-Q drooping control method to balance the system power of the microgrid. Because frequency associates with amplitude recovery, the microgrid voltage frequency is limited to a small range of fluctuations as shown in Figure 17. Besides, the microgrid output power in the whole process is stable, voltage and frequency fluctuations are small in distribution network, as shown in Figure 18. In the grid-connected mode, the microgrid terminal voltage is dictated by the rest of the distribution network, and represents the power system frequency. The microgrid connected with other units contributes to the regulation of the network voltage and frequency. During the whole process, the deviation of the microgrid frequency is less than ± 0.02Hz and the maximum fluctuation of the grid bus voltage is less than ± 0.03%. Both of them meet the requirements of the microgrid.

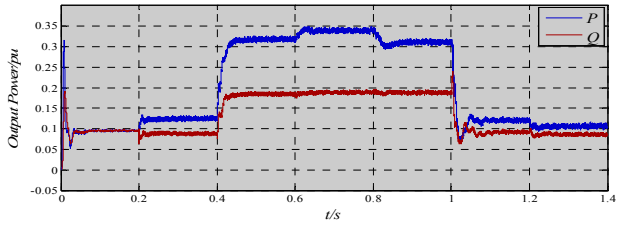

Figure 14. The output power of microsource 1

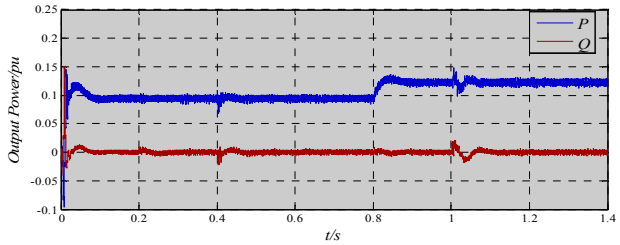

Figure 15. The output power of microsource 2

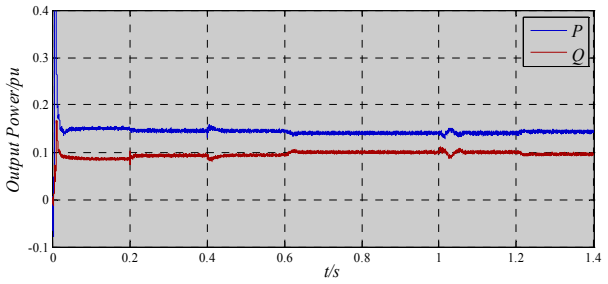

Figure 16. The output power of microsource 3.

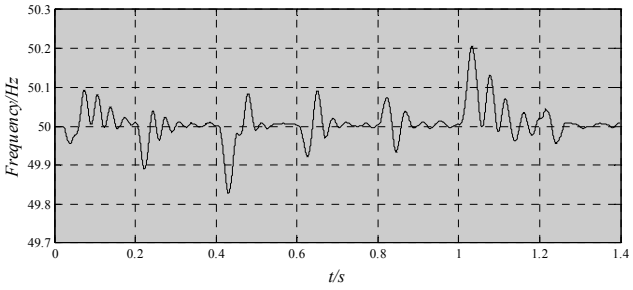

Figure 17. Microgrid voltage frequency

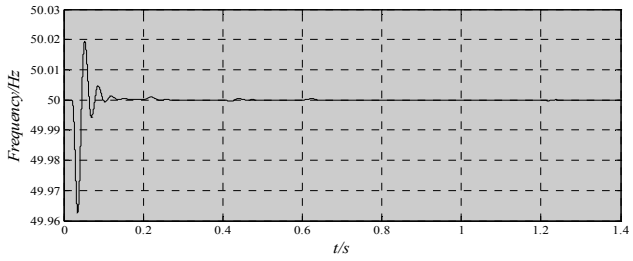

Figure 18. The low voltage distribution network voltage frequency.

VI. CONCLUSION

A power quality dual-loop control strategy for microgrids has been proposed in this paper, it is useful to solve the problems of voltage fluctuations and frequency deviation caused by dramatic change of microsources or loads. First, a feed-forward f-P/V-Q drooping controller is designed to improve the control precision and response speed of the output power of microsources. Second, a control strategy with an external voltage loop and an internal current loop is adopted to solve the coupling between the output active power and reactive power of the inverter.

The proposed control strategy can effectively prevent the shock of the microgrid when microsources or loads change dramatically. The security and stability of the microgrid have been improved. The control strategy can also quickly follow the changes of distribute network voltage and avoided the impact current when the microgrid is connected to the distribution network.

REFERENCES

[1] European Renewable Energy Council, "Renewable energy scenario to 2040: half of the global energy supply from renewables in 2040," May (2004).

[2] G. Pepermans, J. Driesen, D. Haeseldonckx, W. D'haeseleer and R. Belmans, "Distributed generation: definition, benefits and aissues," Energy Policy, 33(6):787-798,(2005).

[3] Lasseter RH, Paigi Paolo, "MicroGrid: a conceptual solution," IEEE Annu Power Electron SpecialistsConf6. 2004(1):4285–4290.

[4] Lasseter RH, "MicroGrids," IEEE Power Eng Soc Transm Distrib Conf. (1):305–308,(2002).

[5] J. A. Peças Lopes, C. L. Moreira, A. G. Madureira, "Defining control strategies for MicroGrids islanded operation," IEEE Trans on Power Systems,21(2):916-924,(2006).

[6] A. L. Dimeas, N. D. Hatziargyriou, "Operation of a multi-agent system for MicroGrid control," IEEE Trans on Power Systems20 (3):1447-1455 , (2005).

[7] A. L. Dimeas, N. D. Hatziargyriou, "Multi-agent based automatic generation control of isolated standalone power system," Power Systems Technology, 1(1):139-14 , (2005).

[8] A.Engler, "Applicability of droops in low voltage grids," International Journal of Distributed Energy Resources, 1(1):1-6, (2005),

[9] Karel De Brabandere, Bruno Bolsens, Jeroen Van den Keybus, Achim Woyte, Johan Driesen, Ronnie Belmans, "A voltage and frequency droop control method for parallel inverters," IEEE Transactions on Power Systems,22(4):1107-1115, (2007).

[10] M.C.Chandorkar, D.M.Divan, R.Adapa, "Control of parallel connected inverters in standalone ac supply systems," IEEE Trans on Industry Applications, 29(1):136-141, (1993).

[11] M.Hauck, H.Spath, "Control of a three phase inverter feeding an unbalanced load and operating in parallel with other power sources," International Power Electronics and Motion Control Conference, Croatia, (2002):p.1-p.10.

[12] J. Matas, Josep M. Guerrero, Luis García de Vicuña, José Matas, Miguel Castilla, Jaume Miret, "A Wireless controller to enhance dynamic performance of parallel inverters in distributed generation system," IEEE Transactions on Industrial Electronics,19(5):1205-1213, (2004).

[13] J. Matas, Josep M. Guerrero, José Matas, Luis García de Vicuña, Miguel Castilla, Jaume Miret, "Wireless-control strategy for parallel operation of distributed-generation inverters," IEEE Transactions on Industrial Electronics, 53(5):1461-1470, (2006).

[14] H. Laaksonen, P. Saari, R. Komulainen, "Voltage and frequency control of inverter based weak LV network Microgrid," International Conference for Future Power Systems, Netherlands, 6 pp, (2005).

[15] R. Majumder, A. Ghosh, G. Ledwich, F. Zare, "Load sharing and power quality enhanced operation of a distributed micro grid," IET Renewable Power Generation,3(2):109-119,(2009).

[16] Mohammad B. Delghavi, Amirnaser Yazdani, "An Adaptive Feedforward Compensation for Stability Enhancement in Droop-Controlled Inverter-Based Microgrids," IEEE Transactions on Power Delivery, 26(3):1764-1773, (2011).

[17] Robert H. Lasseter, "Control and Design of Microgrid Components,"http://www.pserc.wisc.edu/documents/publications/reports/2006_reports/lasseter_microgridcontrol_final_project_report.pdf.

[18] WANG Chengshan, XIAO Zhaoxia, WANG Shouxiang, "Synthetical Control and Analysis of Microgrid," Automation of Electric Power Systems, 32(7): 98-103, (2008)